1999-06-01

Fusion neutron transient effects to charge coupled device camera images

Giauque, Michael S.

Monterey, California. Naval Postgraduate School

NAVAL POSTGRADUATE SCHOOL
Monterey, California

THESIS

FUSION NEUTRON TRANSIENT EFFECTS TO CHARGE COUPLED DEVICE CAMERA IMAGES

by

Michael S. Giauque

June 1999

Thesis Advisor: William B. Maier II
Thesis Co-advisor: D. Scott Davis

REPORT DOCUMENTATION PAGE

Form Approved
OMB No. 0704-0188

1. AGENCY USE ONLY *(Leave blank)*	2. REPORT DATE June 1999	3. REPORT TYPE AND DATES COVERED Master's Thesis

4. TITLE AND SUBTITLE
FUSION NEUTRON TRANSIENT EFFECTS TO CHARGED COUPLED DEVICE CAMERA IMAGES

5. FUNDING NUMBERS

6. AUTHOR(S)
Giauque, Michael S.

7. PERFORMING ORGANIZATION NAME(S) AND ADDRESS(ES)
Naval Postgraduate School
Monterey, CA 93943-5000

8. PERFORMING ORGANIZATION REPORT NUMBER

9. SPONSORING / MONITORING AGENCY NAME(S) AND ADDRESS(ES)

10. SPONSORING / MONITORING AGENCY REPORT NUMBER

11. SUPPLEMENTARY NOTES
The views expressed in this thesis are those of the author and do not reflect the official policy or position of the Department of Defense or the U.S. Government.

12a. DISTRIBUTION / AVAILABILITY STATEMENT
Approved for public release; distribution is unlimited.

12b. DISTRIBUTION CODE

13. ABSTRACT ***(maximum 200 words)***

A charge coupled device (CCD) camera's images were degraded by neutron-induced blemishes, called stars, while being irradiated with 14 MeV neutrons (n) from the Rotating Target Neutron Source. This thesis analyzed simulated images for a CCD camera operating during neutron irradiation. The simulated images were created to provide data to help determine how much shielding a CCD camera would require while being used a diagnostic tool during inertial fusion events at the National Ignition Facility. The simulated images were created from data obtained at the Rotating Target Neutron Source. The Contrast Transfer Function (CTF), autocorrelation function and visual comparisons were used as measures of the transient effects of the neutron irradiation on the simulated images. The CTF and visual image quality started to degrade significantly at neutron fluences around 10^8 n/cm^2. The autocorrelation function determined that the average size of neutron-induced star was 4 x 4 pixels. Increasing neutron fluence produced image changes that could be explained by a variation in sensitivity across the camera face or (more likely) by increased Charge Transfer Inefficiency (CTI) with increasing charge loading of the CCD.

14. SUBJECT TERMS Neutron Irradiation, Charge Coupled Device Camera, Contrast Transfer Function	15. NUMBER OF PAGES 57
	16. PRICE CODE

17. SECURITY CLASSIFICATION OF REPORT	18. SECURITY CLASSIFICATION OF THIS PAGE	19. SECURITY CLASSIFICATION OF ABSTRACT	20. LIMITATION OF ABSTRACT
Unclassified	Unclassified	Unclassified	UL

Approved for public release; distribution is unlimited

FUSION NEUTRON TRANSIENT EFFECTS TO CHARGE COUPLED DEVICE CAMERA IMAGES

Michael S. Giauque
Lieutenant Commander, United States Navy
B.S., U.S. Naval Academy, 1986

Submitted in partial fulfillment of the
requirements for the degree of

MASTER OF SCIENCE IN APPLIED PHYSICS

from the

NAVAL POSTGRADUATE SCHOOL
June 1999

ABSTRACT

A charge coupled device (CCD) camera's images were degraded by neutron-induced blemishes, called stars, while being irradiated with 14 MeV neutrons (n) from the Rotating Target Neutron Source. This thesis analyzed simulated images for a CCD camera operating during neutron irradiation. The simulated images were created to provide data to help determine how much shielding a CCD camera would require while being used a diagnostic tool during inertial fusion events at the National Ignition Facility. The simulated images were created from data obtained at the Rotating Target Neutron Source. The Contrast Transfer Function (CTF), autocorrelation function and visual comparisons were used as measures of the transient effects of the neutron irradiation on the simulated images. The CTF and visual image quality started to degrade significantly at neutron fluences around 10^8 n/cm^2. The autocorrelation function determined that the average size of neutron-induced star was 4 x 4 pixels. Increasing neutron fluence produced image changes that could be explained by a variation in sensitivity across the camera face or (more likely) by increased Charge Transfer Inefficiency (CTI) with increasing charge loading of the CCD.

TABLE OF CONTENTS

LIST OF SYMBOLS

A	Area of a pixel
b	Digital bias offset
c_e	Charge transfer efficiency
g	Gain
J	Dark current
n	Neutron
n	Total number of rows
q	Magnitude of electronic charge
R_j	Average digital value of the j^{th} row of pixels
t	Total time of irradiation run
t_e	Exposure time
t_r	Readout time

ACKNOWLEDGEMENT

The author wants to thank Prof. William Maier, Prof. Scott Davis, Prof. Don Walters, and Prof. Andrés Larraza of the Naval Postgraduate School for their help and guidance; Mr. Craig Sangster of Lawrence Livermore National Laboratories for his guidance; and Breckenridge Morgan Sr. for his constant help on computers, software and thesis construction.

I. INTRODUCTION

Construction of the National Ignition Facility (NIF) is well underway at the Lawrence Livermore National Laboratory (LLNL). The two main reasons for constructing the NIF are to maintain the competency of scientists involved with the physics of nuclear weapons for the Department of Energy's Stockpile Stewardship Program and to conduct experiments to help determine if inertial fusion can be used as a clean source of energy. NIF will conduct experiments by igniting deuterium-tritium (DT) fuel pellets with high power lasers. The conditions produced will be similar to those which occur in the sun and nuclear explosions.

The thermonuclear fusion reaction of DT yields a 14 MeV neutron, a 3 MeV alpha particle and 17 MeV of kinetic energy:

$$D + T \rightarrow \alpha + n + 17MeV\,.$$

Diagnostics are required to monitor this reaction and others that occur in the NIF reaction chamber. The charge coupled device (CCD) camera is one proposed diagnostic device.

The purpose of this thesis research was to analyze images taken during Rotating Target Neutron Source (RTNS) irradiation and to create simulated irradiated images to demonstrate how the transient damage effects of neutron irradiation would affect CCD imaging of experiments in the NIF. A secondary goal was to analyze the illuminated bench images to determine if camera sensitivity was effected by the neutron irradiation.

II. BACKGROUND

In work conducted as a predecessor to this thesis research, LT Chris Amaden observed effects produced by irradiation of a CCD camera by 14 MeV neutrons at the Rotating Target Neutron Source (RTNS). His analysis concentrated on the cumulative permanent damage to the camera. The results of the damage included increases in dark current and charge transfer inefficiency (CTI) and a decrease in Contrast Transfer Function (CTF) with increasing neutron fluence damage. The effect of lowering the camera temperature on the amount of dark current generated was also observed. His analysis was derived from images taken during bench tests before and after periods of irradiation by the RTNS. Because this thesis is based on his data, a detailed description of his experiment and results is given in this section [1].

A. PRIOR RESEARCH

1. Charge-Coupled Device (CCD) Camera

The CCD camera is used in many scientific applications because it has good spatial resolution and sensitivity to small light signals. The CCD is an array of silicon detectors which form potential wells by application of potentials to insulated gates trapping electrons generated from light falling on the arrays over a period of time. The number of electrons generated is proportional to the amount of light flux falling on the semiconductor [2].

When the period of exposure to light is completed, the controller will read out the array, converting the charge value associated with the electrons in each potential well into a digital value. The method used to read out the image by the camera used in this experiment consists of the following: each row of pixels in the image is transferred into a readout register, then each pixel charge in the row is read out, digitized and stored

individually. Then next row of pixels in the image is then transferred to the readout register, and so forth, until the entire image is read out row by row.

The camera and controller used in this experiment were both manufactured by Princeton Instruments. The camera had an EEV 1152 x 1242 CCD pixel array and used a ST-138 controller. The camera controller's main function was to take the analog signal from the camera and convert it to digital information. During image readout the data was digitized in 16-bit format so the highest value (saturation) was 65535 (white) and the lowest was zero (black). The controller also provided power, timing and commands to the camera. The commercial software, *IPLab Spectrum* version 3.1, was used to run the camera/controller package through scripting. Scripting (creating macros from known commands) allowed the operator to sequence commands to the camera/controller or apply a sequence of steps to process images.

2. Rotating Target Neutron Source (RTNS)

The RTNS produced 14 MeV neutrons, from the DT fusion reaction shown previously. The neutrons produced by the RTNS were used to irradiate the CCD camera for radiation damage studies. The neutrons are produced by accelerating a beam of deuterons to an energy $\leq$ 399 keV with currents in the 2-5 mA range at an internally cooled, rotating, tritium target. The maximum rate of neutrons the RTNS can produce is 1.0×10^{12} n/sec. Figure 1 is a diagram of the main RTNS components. The RTNS was located in the basement at Etcheverry Hall on the University of California, Berkeley campus [3].

3. *IPLab Spectrum* (Software)

IPlab Spectrum is a general image processing and analysis tool. This software was used initially to control the camera/controller to capture images taken with the camera during the experiment. It was later used to process and to analyze images in the

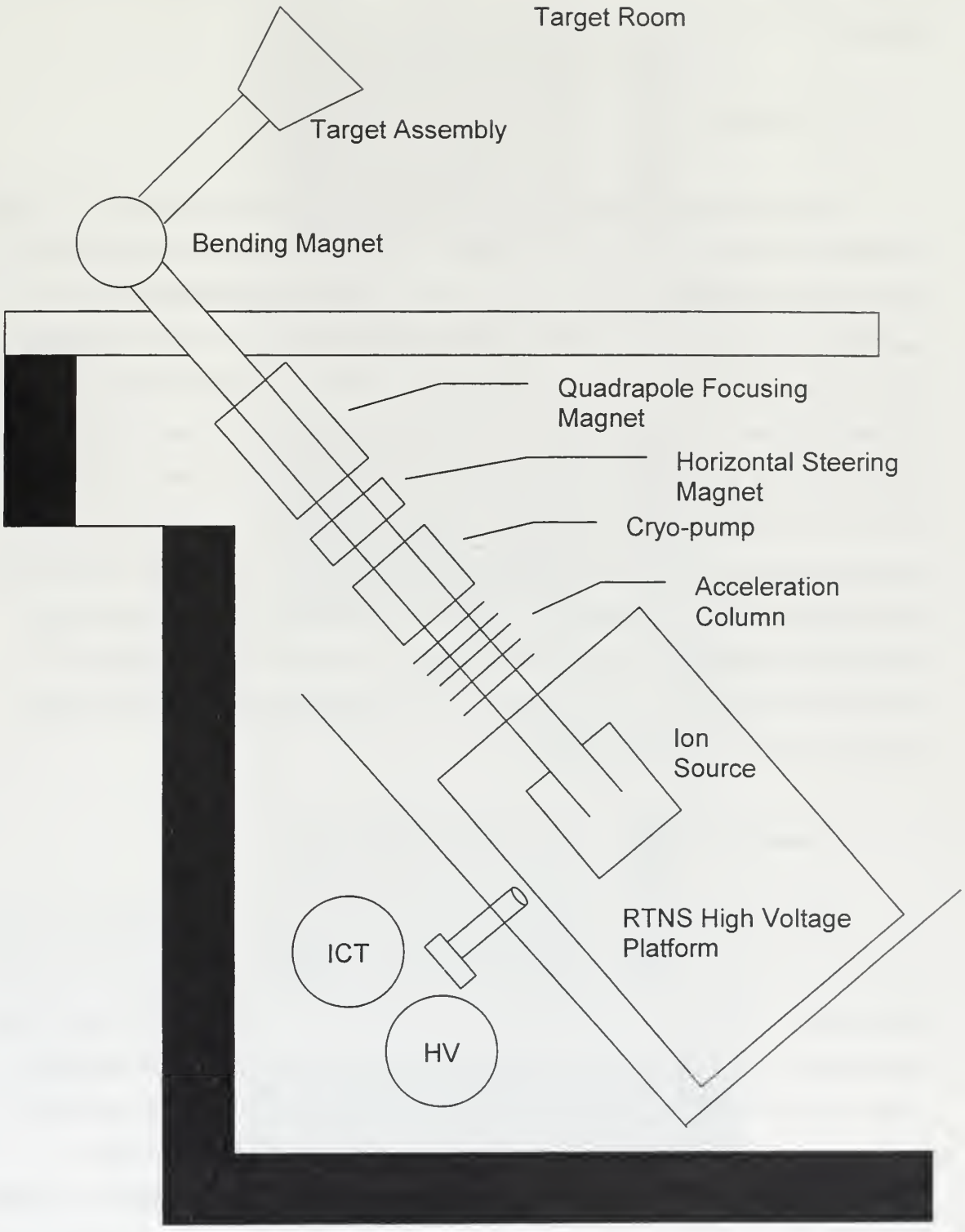

Figure 1. RTNS layout.

initial thesis research conducted by LT Amaden as well as the further analysis of the images, taken during neutron irradiation, covered in this thesis.

4. The Experiment

The experiment was conducted by LT Amaden over ten days in March 1997 at the University of California, Berkeley. The camera and controller were provided by LLNL and the equipment for high-resolution imaging was provided by the Bechtel Nevada Laboratories. The experiment involved irradiating the camera for a period of time and then moving it to a bench to take a series of images. The bench-imaged targets consisted of black fields(no external light), white fields (illuminated), and illuminated high-resolution slides (see Figure 2). During bench imaging, the camera was mounted on a 500-mm Gaertner rail along with the lens, filters, slides and flash. A flashhead with an optiliner barrel provided a uniform source of white light when desired. This light would pass through a lens for focussing, filters and finally through a slide. The camera was transferred to the radiation chamber for the irradiated images and was mounted on a wooden ladder placed at different distances from the neutron source depending on the amount of neutron irradiation desired.

5. Data Collection

The array size chosen by LT Amaden for the images was 400 x 1000 pixels out of an 1152 x 1242 array. This smaller array was chosen to avoid fault lines in the array face of the camera. Through experimentation the readout time t_r of the 400 x 1000 array was determined to be 1.22 seconds. The total time the image was exposed to radiation was determined by adding t_r to the exposure time t_e. Besides the bench images, a series of images were taken during neutron irradiation and saved to the hard drive of the controlling computer each time the camera was exposed to the RTNS irradiation. Images

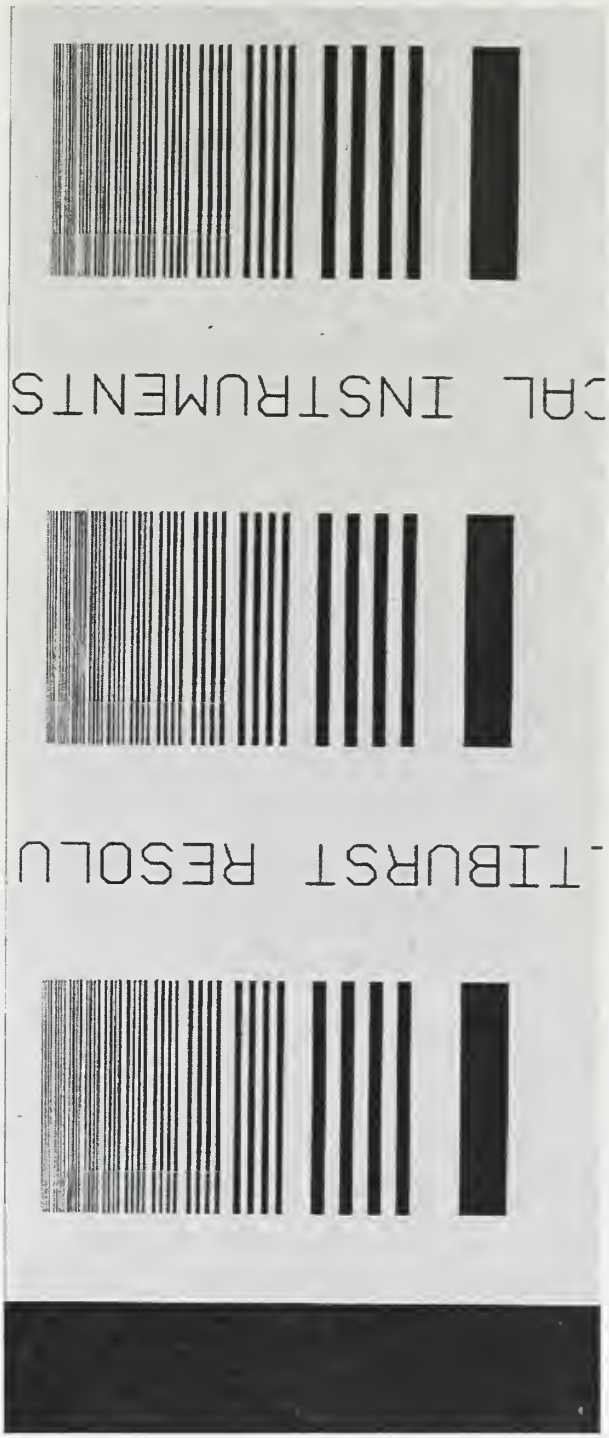

Figure 2. Image of high-resolution slide before neutron irradiation.

taken both on the bench and in the radiation chamber were either 1ms or 400 ms exposures.

B. PREVIOUS DATA AND DEFINITIONS

1. Damage Mechanisms

The basic mechanisms for neutron radiation damage to silicon CCDs are total ionizing dose effects, displacement damage and transient effects. The CCD was protected from charged particles with an aluminum shield plate, so the total ionizing dose effects were kept to a minimum. Collisions between the neutrons and atoms in the silicon lattice of the CCD caused the displacement of silicon atoms from their lattice sites. The resulting damaged areas increased the generation of dark current and caused the trapping of signal charges, which interfered with the charge transfer process. The final type of damage, which was of primary interest in this thesis research, were the transient effects that caused the speckling of the CCD image shown in Figure 3. The speckled portions of the images have been nicknamed stars. [4].

2. Contrast Transfer Function (CTF)

LT Amaden used the contrast transfer function (CTF) as a method of measuring the resolution of square wave bar patterns seen on the high-resolution slide image (Figure 2). He defined the CTF as:

$$CTF = \frac{B_{\max} - B_{\min}}{B_{\max} + B_{\min}}, \tag{1}$$

where $B_{\min} \equiv$ the minimum digital value and $B_{\max} \equiv$ the maximum digital value from the column-averaged four pixel-wide bars in the middle bar set of the high-resolution slide

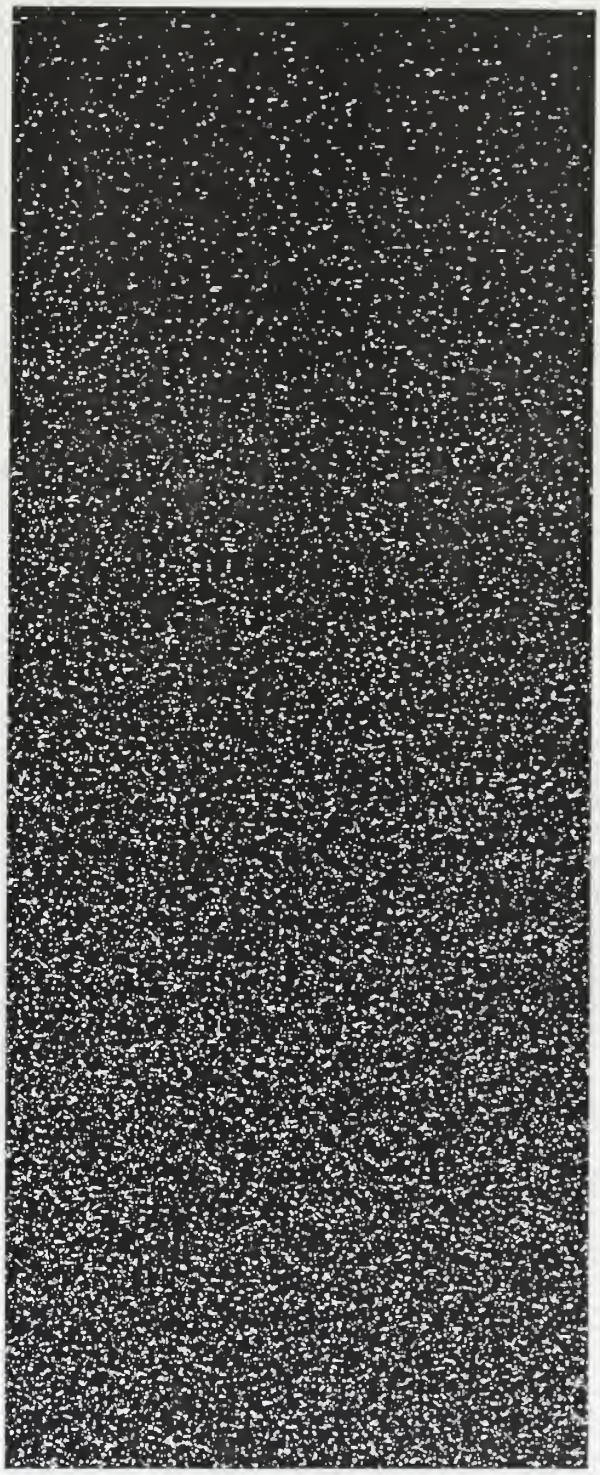

Figure 3. Neutron transient effects (Stars). Neutron fluence was 2.1×10^8 n/cm^2 at the top and 7.8×10^8 n/cm^2 at the bottom of image.

(Figure 2), third set of bars from the right. The high-resolution slide image had 10 sets of four bars and one large bar in each of the three patterns located at the top, middle and bottom of the image. The CTF was measured in the four pixel-wide bar set because bar sets less than this tended to be too close to the sampling size, 1 pixel, and larger bar sets did not show as much degradation. The designated region of interest (ROI) of each image included only the center bar set. Using *IPLab*, an average was calculated for each column in the ROI, which created a graph like the one shown in Figure 4. The *IPLab* view was then changed to view data, which gave a digital value for the average of each column. The minimum and maximum digital values for the four-pixel wide bar set were located and used in the CTF.

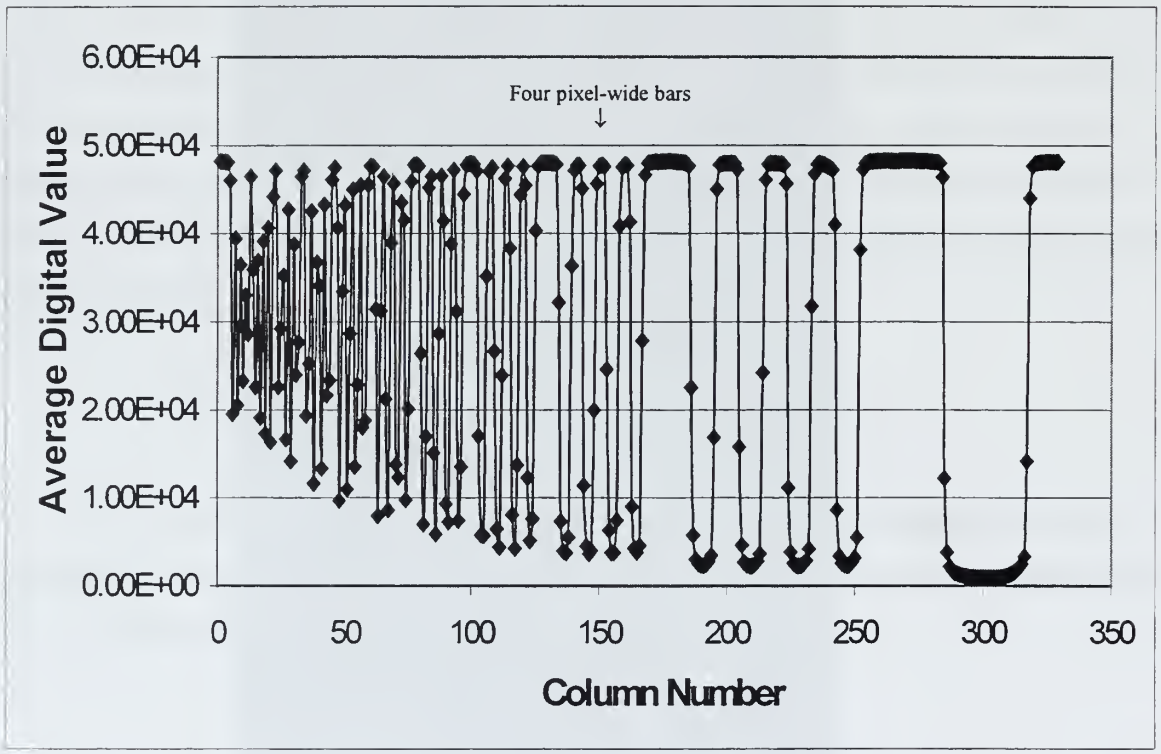

Figure 4. Graph of average digital value for columns in a bar pattern.

LT Amaden used this measure to show the effects of dark current and temperature on the camera imaging resolution. I will use the CTF later to compare the loss of resolution due to transient effects to the losses due to dislocation damage and temperature effects.

3. Charge Transfer Inefficiency (CTI)

The CTI is defined as CTI = 1-CTE where CTE is the charge transfer efficiency. CTE is the fraction of the initial charge stored in a CCD pixel that is transferred to an adjacent pixel. CTI is the fraction of initial charge left behind in a carrier well when the charge is moved from one pixel element to the next. Even in the absence of neutron irradiation, CTI is affected by the temperature, the number of interface states, and the charge loading of the pixels.

Interface states are continuously distributed energy states in the bandgap of semiconductor/oxide interface of the detector and are increased by the neutron displacement damage. These interface states affect CTI by slowing the rate of charge transfer by capturing or trapping charge and emitting it at a slower rate than non-captured charges. The displacement damage discussed previously causes an increase in the number of interface sites and an increase in the CTI [4].

LT Amaden calculated the CTI for the various fluences used in the experiment. He used the following equation to show the effects of CTI on the CCD average row digital value:

$$R_j = \frac{A}{qg}\left[Jt_e\left(c_e\right)^j + J\frac{t_r}{n-1}\frac{c_e - \left(c_e\right)^j}{1-c_e}\right] + b,$$

where R_j was average digital value of the j^{th} row of pixels, A was area of pixel, q was the magnitude of electronic charge, g was gain, J was dark current, c_e was CTE, and b was the digital bias offset. Figure 5 was a plot he made showing the CTI vs fluence. A CTI

along a trendline of the data below a fluence of 10^{10} n/cm^2 in Figure 10 was approximately 1.8 x 10^{-4} and corresponds to a CTE of 0.99982 $\pm$ 00003.

LT Amaden treated the charge left behind as if it was lost, because the observed standard deviation of residual charge fluctuations, with a mean charge value around 5x10^4 was about 100. The amount of charge left behind during a typical charge transfer due to CTI was (5 x 10^4) x .00018 = 9. Although a CTI of 9 was insignificant statistically when compared to the typical fluctuation size of 100, this charge would be important in this thesis research due to its effect on determining camera sensitivity.

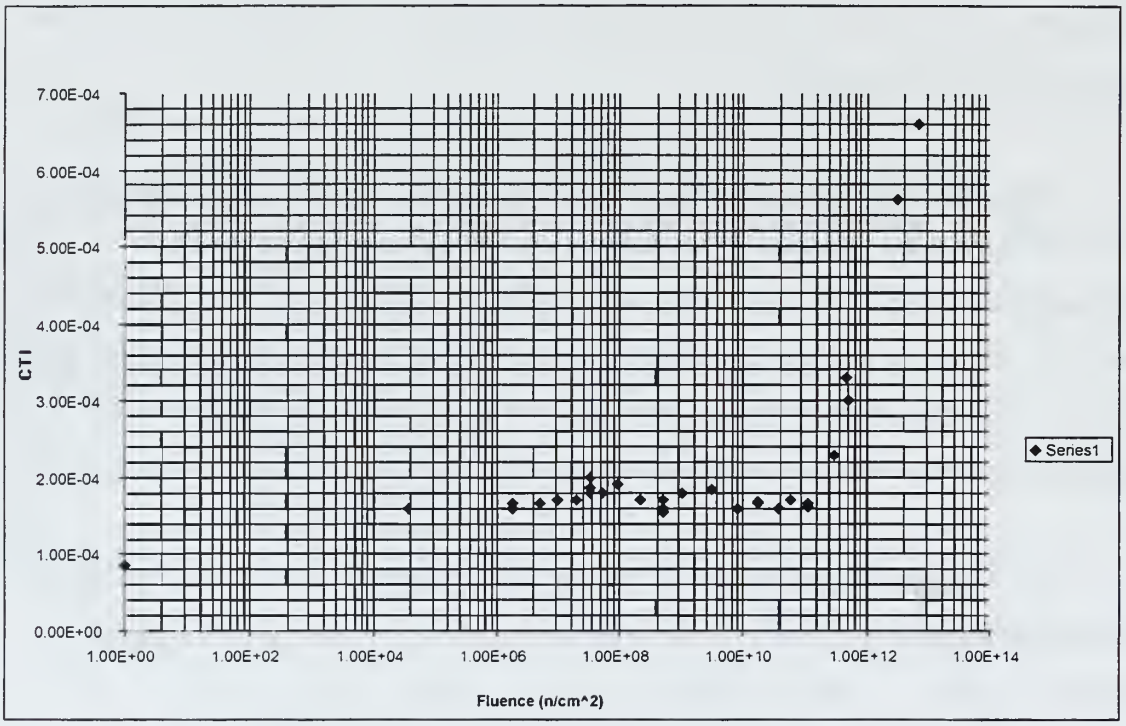

Figure 5. CTI vs. fluence. This semilog plot shows the relationship of CTI with fluence from Ref [1].

III. TRANSIENT EFFECTS ANALYSIS

The transient effects of interest here are the speckling of the CCD image taken during irradiation as shown in Figure 3. The speckles are called stars and are caused by the induced charge created by the neutrons passing through the active region of a detector. The effects are called transient because this extra charge was transferred out when the image was read out. This charge generally overflowed single pixel potential wells, so groups of adjacent pixels would carry excess charges for a single neutron event. The rows of pixels would continue to be susceptible to transient effects of neutron irradiation during the 1.22 sec readout. The last pixels read out, the bottom of Figure 3, exhibited an increasing density of neutron events (stars).

A. FLUENCE LEVELS

1. Fusion

I generated realistic images showing the transient effects of neutron interactions produced during fusion by using the images obtained during the RTNS irradiation of the camera. The amounts of neutrons produced in fusion reactions, for both a "good" burn and a "dud," were required to determine the fluence desired in the created images. Tables 1 and 2 were taken from a paper written at LLNL with a "good" burn represented by the 21.8 Megajoule (MJ) data and the "dud" by the 1.9 MJ data. This data was based upon a 1 ns full-width half maximum pulse of radiation[5]. Creating images with values of fluence similar to these and showing how the various fluences would effect a high-resolution slide image has been the goal of this research.

	Source	Inside TC	Inside TC	Outside TC	Inside TR
Distance from NIF Target	0 Meters	2.5 Meters	5.0 Meters	5.5 Meters	13 Meters
Neutron Fluence (n/cm^2)	1.00×10^{19}	1.27×10^{13}	3.18×10^{12}	1.00×10^{11}	2.00×10^{10}

Table 1. 21.8 Megajoule shot after Ref [5].

	Source	Inside TC	Inside TC	Outside TC	Inside TR
Distance from NIF Target	0 Meters	2.5 Meters	5.0 Meters	5.5 Meters	13 Meters
Neutron Fluence (n/cm^2)	3.56×10^{16}	4.50×10^{10}	1.12×10^{10}	4.20×10^{8}	8.40×10^{7}

Table 2. 1.9 Megajoule shot (Dud) after Ref [5].

2. RTNS Flux

Calculating the amount of fluence that was imaged during one exposure required the determination of flux produced by the RTNS during the run in which the image was taken. During the experiment, values of total fluence were documented and added after every irradiation. A chart of these values is shown in Table 3. It shows the run number, the date and the integrated neutron fluence the camera had accumulated during that run. The fluence values were obtained by using deuteron current correlation for fluences less than 10^7 n/cm^2 and activation results of Ni-57 for all other irradiations[1]. The flux could be determined from the fluence for that run by dividing the fluence by the time of the run.

The flux value was then multiplied by the sum of the exposure and readout times to calculate the neutron fluence for the particular image.

$$\left(\frac{\text{total run fluence}}{t}\right)\cdot\left(t_e + t_r\right) = \text{image fluence}\cdot$$

The maximum neutron flux created by the RTNS in these runs was $5.83\text{x}10^8$ n/cm^2-sec. Therefore, the maximum fluence in a 1 ms exposure is $7.17\text{x}10^8$ n/cm^2, and the maximum for a 400 ms exposure was $9.45\text{x}10^8$ n/cm^2, both values based on the maximum neutron flux of the RTNS during the final irradiation run.

Table 2 predicts that a direct path image of a "dud" shot at 13 meters would be exposed to a fluence of about $8.40\text{x}10^7$ n/cm^2. While an exposures made during the last few RTNS runs could produce an image with greater fluence than the "dud," the large dark current

Run Number	Date Time March 1997	Fluence n/cm^2	Run Number	Date Time March 1997	Fluence n/cm^2
1	13 3.5 min	$3.80\text{x}10^4$	12	17 10.0 min	$2.00\text{x}10^9$
2	13 3.25 min	$1.77\text{x}10^6$	13	17 12.5 min	$5.10\text{x}10^9$
3	14 5.38 min	$3.30\text{x}10^6$	14	17 10.0 min	$8.90\text{x}10^9$
4	14 6.13 min	$4.70\text{x}10^6$	15	18 18.45 min	$2.00\text{x}10^{10}$
5	14 5.00 min	$1.00\text{x}10^7$	16	18 25.0 min	$2.40\text{x}10^{10}$
6	14 5.32 min	$1.30\text{x}10^7$	17	18 55.0 min	$4.90\text{x}10^{10}$
7	15 8.13 min	$1.80\text{x}10^7$	18	19 165 min	$1.80\text{x}10^{11}$
8	15 15.0 min	$3.90\text{x}10^7$	19	20 12.0 min	$1.80\text{x}10^{11}$
9	15 10.3 min	$1.30\text{x}10^8$	21	20 90.0 min	$2.60\text{x}10^{12}$
10	15 10.3 min	$2.80\text{x}10^8$	22	21 100 min	$3.50\text{x}10^{12}$
11	17 10.7 min	$5.00\text{x}10^8$			

Table 3. Run number and fluence per run.

created by the permanent damage to the camera made many of the images from these later runs impossible to use in this thesis research.

Images for higher fluence were simulated in this thesis research by adding images for lesser fluences because levels higher than 7.8×10^8 n/cm^2 were not available. These images for higher fluence were created to show the transient effects of the neutrons on the high-resolution slide image.

B. SIMULATED IMAGE CREATION

The image arithmetic function in *IPLab* allowed images of identified dimensions to be added, subtracted, multiplied or divided. There were various levels of dark current generated during the irradiation runs. The permanent damage from the irradiations added up so that the integrated dark current increased as the experiment proceeded. To remove the effects of the dark current, the process of taking an irradiated image and subtracting an image taken in the dark from a bench run just before or after the irradiation run would remove most of the excess dark current from the irradiated picture. This procedure allowed one to see more of the transient effects caused during irradiation rather than the saturation caused by the dark current. Some images taken during the final runs were unusable due to the high degree of saturation caused by dark current. If this large amount of dark current was removed from these saturated images by subtraction, too much of the image was lost to show the transient effects of the neutrons. The irradiated images from different runs were then added to the high-resolution image taken before irradiation began. The procedure is shown in Figure 6.

To create an image with fluence evenly distributed from top to bottom, an irradiated image would be vertically flipped and added to the unflipped image. The fluence for this image was calculated by adding the fluence at the top corner where the

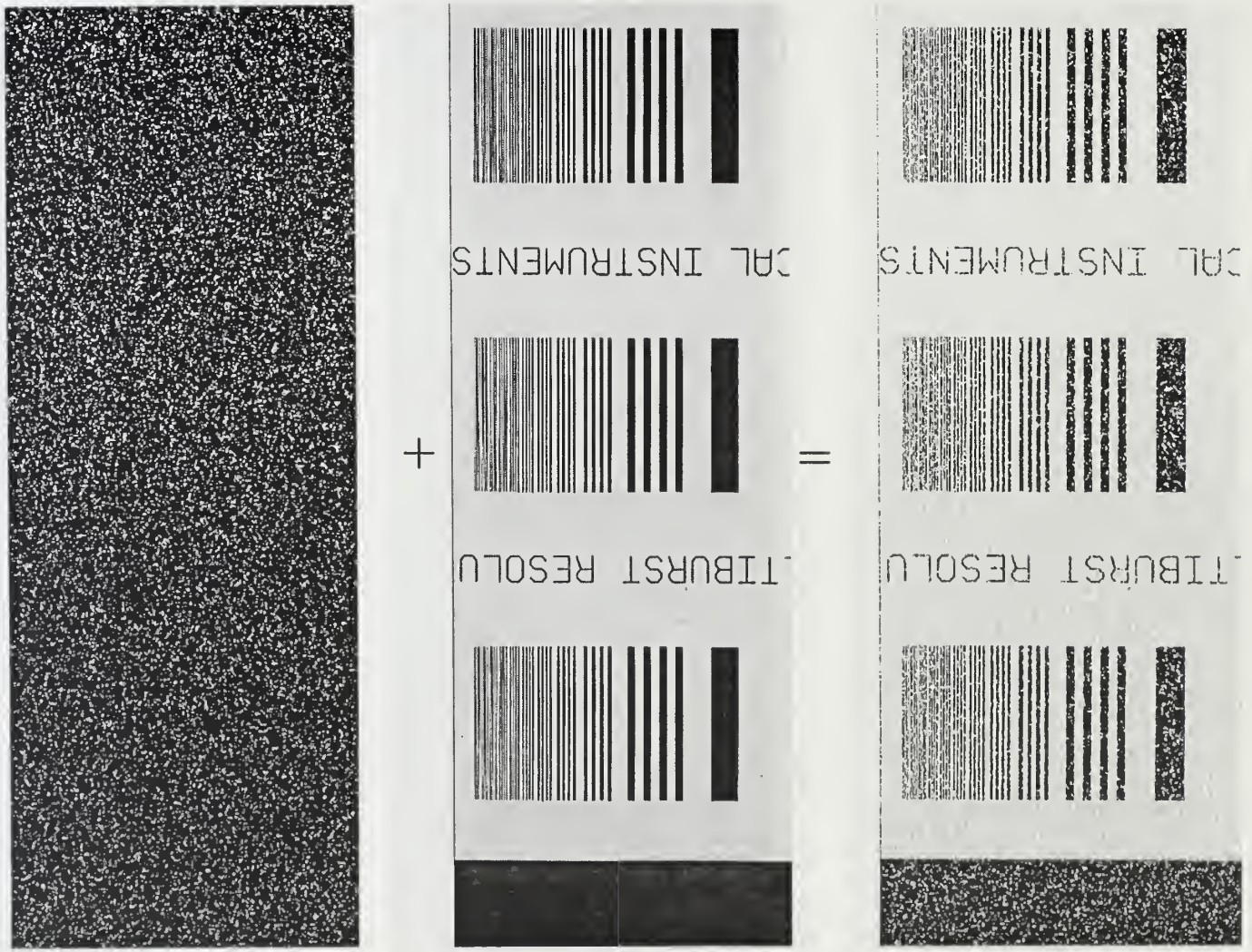

Figure 6. Image addition example.

first pixel was read out and the fluence of last pixel read out at the bottom of an image like Figure 3. The top row of an image taken during the 21st run had a fluence of 2.12×10^8 n/cm^2 with the last row exposed to a fluence of 7.8×10^8 n/cm^2, resulting in an overall fluence of 9.92×10^8 n/cm^2. The variation in star density is eliminated by this procedure. Uniform neutron irradiation is close to what will be seen in the target area during fusion because that event will only take a few nanoseconds and will appear to be an instantaneous event to the camera. Figure 7 shows the result of adding an irradiated image and its inverted image.

Next, simulated images created for various neutron fluences were laid on the high-resolution slide image to show the effects of fluences corresponding to those described in Tables 1 and 2. Figure 2 is reproduced as Figure 8 so that it can be compared to the simulated irradiated pictures. Figure 9 is a simulated image of a fluence that is 2.12×10^8 n/cm^2 at the top and 7.8×10^8 n/cm^2 at the bottom. Figure 10 corresponds to a fluence of 9.92×10^8 n/cm^2, distributed evenly, a result of adding the inverted fluence image to the image used in Figure 9. Figure 11 was obtained by adding a horizontally flipped image of the fluence used in Figure 10 and corresponds to a fluence of 1.98×10^9 n/cm^2, also distributed evenly, and has twice the fluence of the Figure 10 image. Figure 11 is not a bad photocopy of an image, it is washed out from the density of stars produced at this fluence. A 21.8 Megajoule fusion burn is expected to produce a fluence of 2×10^{10} n/cm^2 at 13 m (Table 1), over an order of magnitude greater than that for the highest fluence image in Figure 9.

C. CREATED IMAGE VISUAL RESULTS

The images created showed that there were significant visual effects on the image of the high- resolution slide. These effects would preclude using the camera in a direct path within 13 m for the fusion event. The camera will need to be placed off-axis with shielding arranged to reduce the CCD's exposure to neutron fluence significantly. The

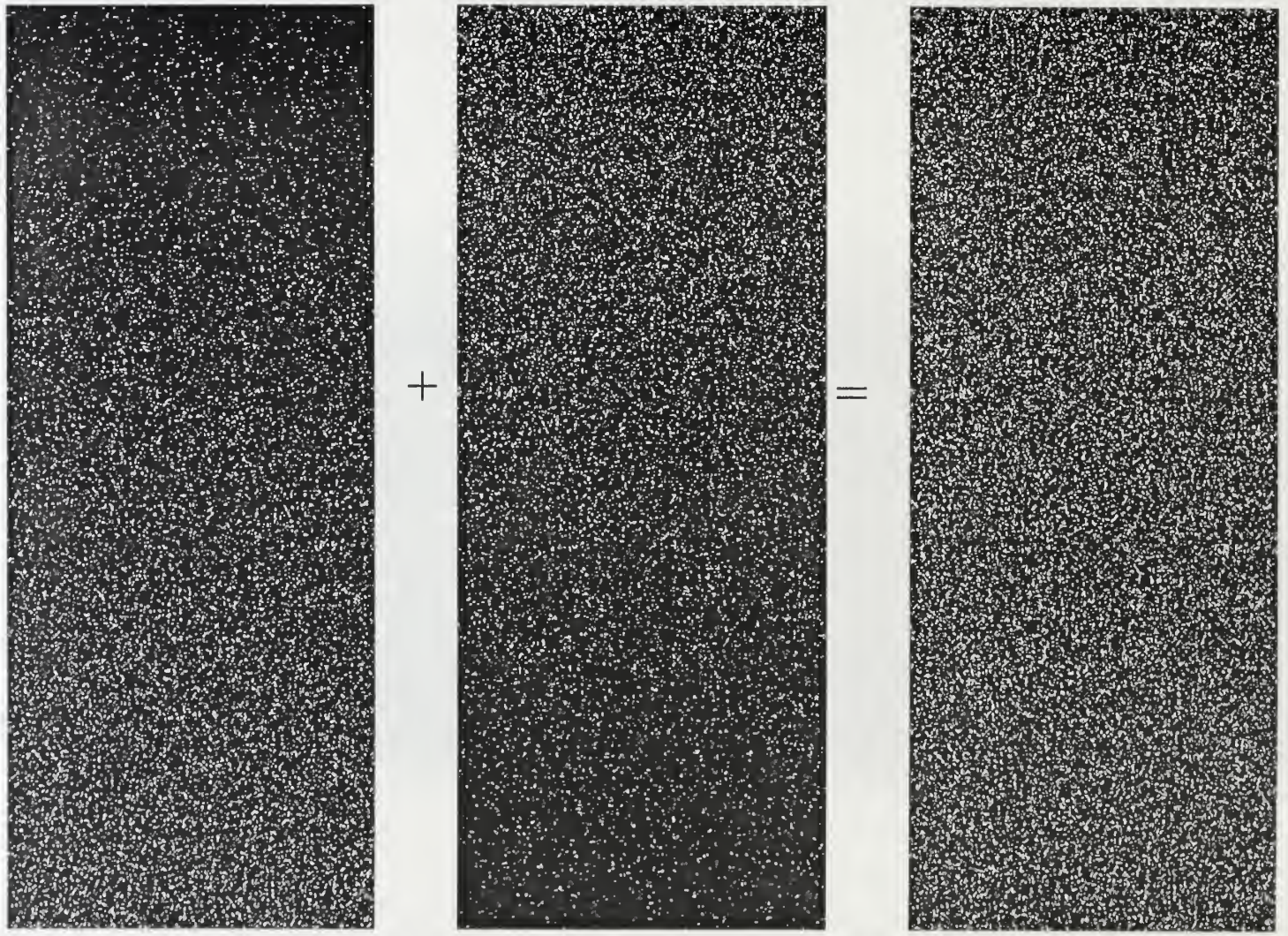

Figure 7. Image plus inverted image resulting in a fluence of 9.92×10^8 n/cm^2

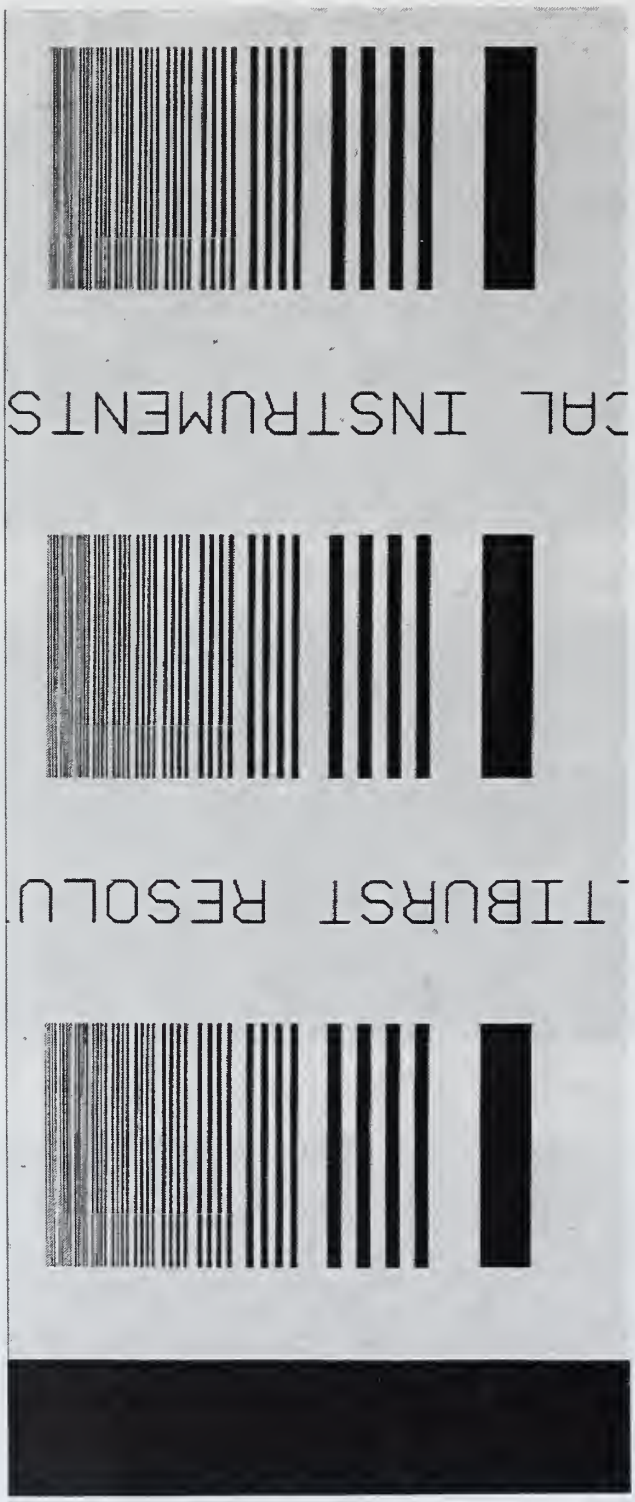

Figure 8. High-resolution slide image.

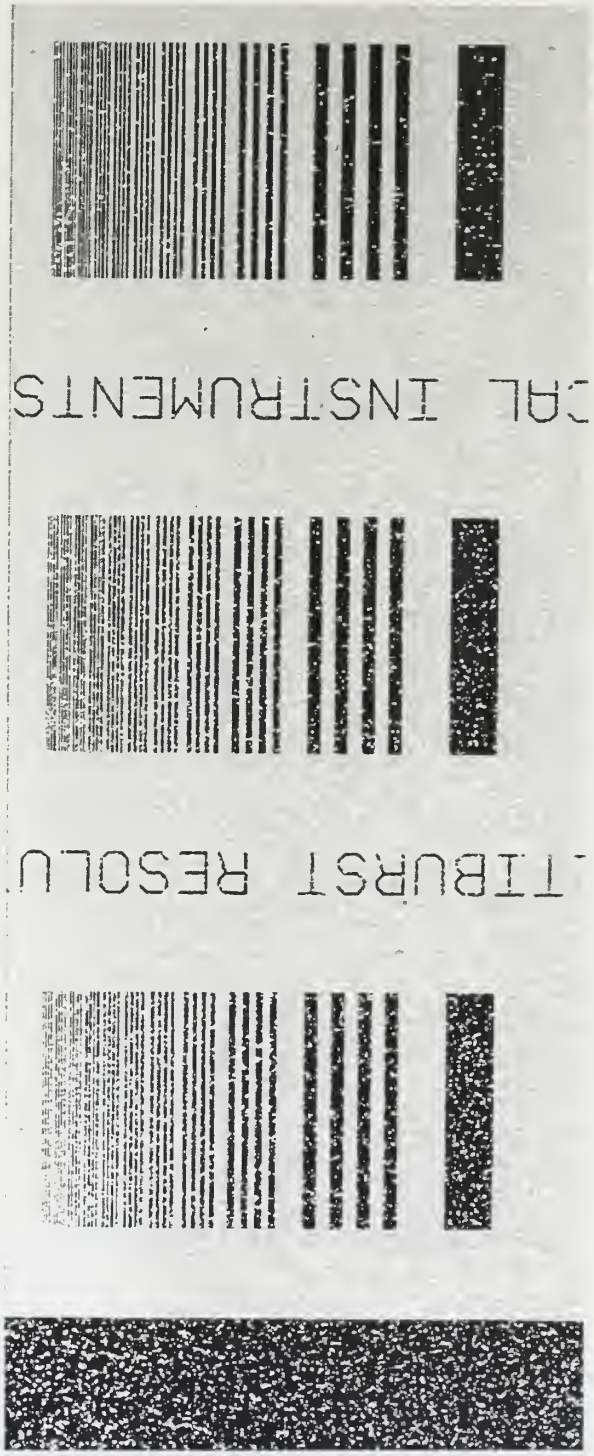

Figure 9. Image corresponding to a density of stars increasing from a fluence of 2.12×10^8 n/cm^2 at the top to 7.8×10^8 n/cm^2 at the bottom.

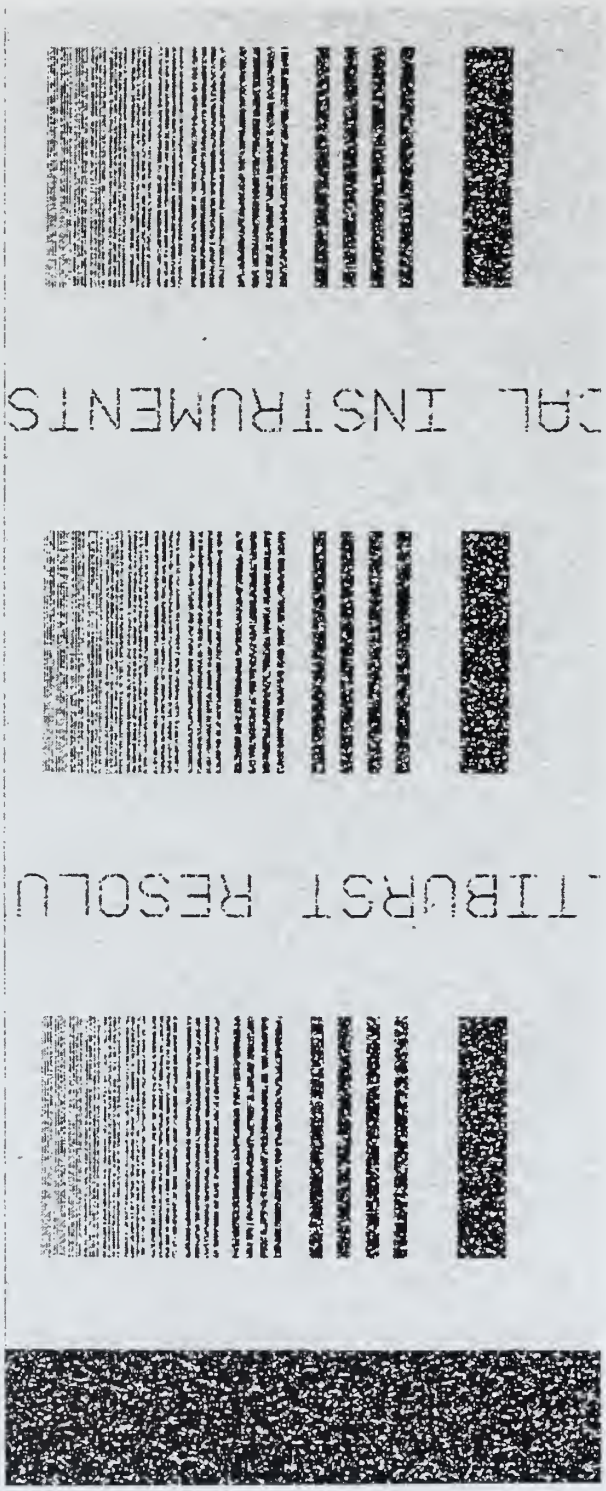

Figure 10. Image with fluence corresponding to 9.92×10^8 n/cm^2.

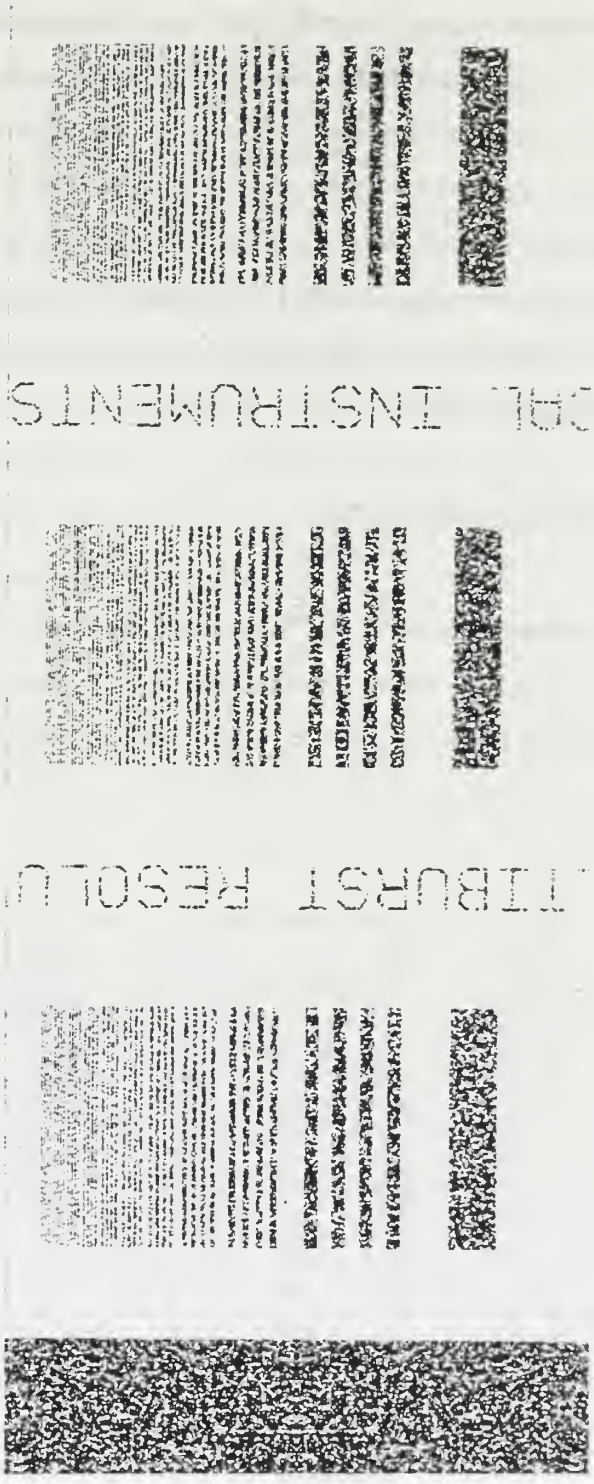

Figure 11. Image with fluence corresponding to 1.98×10^9 n/cm^2.

images in this thesis research were all created as if it were the camera's first exposure to the neutron fluence with no previous permanent damage to the camera. As Ref [1] indicated, a lower temperature and shielding may also decrease the amount of permanent damage from dislocations and dark current production. The set of images in Appendix A show what the visual effects are estimated to be for some fluences lower than $1.0x10^8$ n/cm^2. These images and the results of Ref [1] can be used to help make decisions on how much shielding of neutron fluence is required, and at what temperature, for acceptable images and camera life.

D. CONTRAST TRANSFER FUNCTION

A comparison was made between CTF plots, one calculated based on dark current and temperature effects (Ref [1]), and the other on the stars produced by the transient effects. Figure 12 shows the plot of CTF versus fluence from Ref [1]. This figure gives a

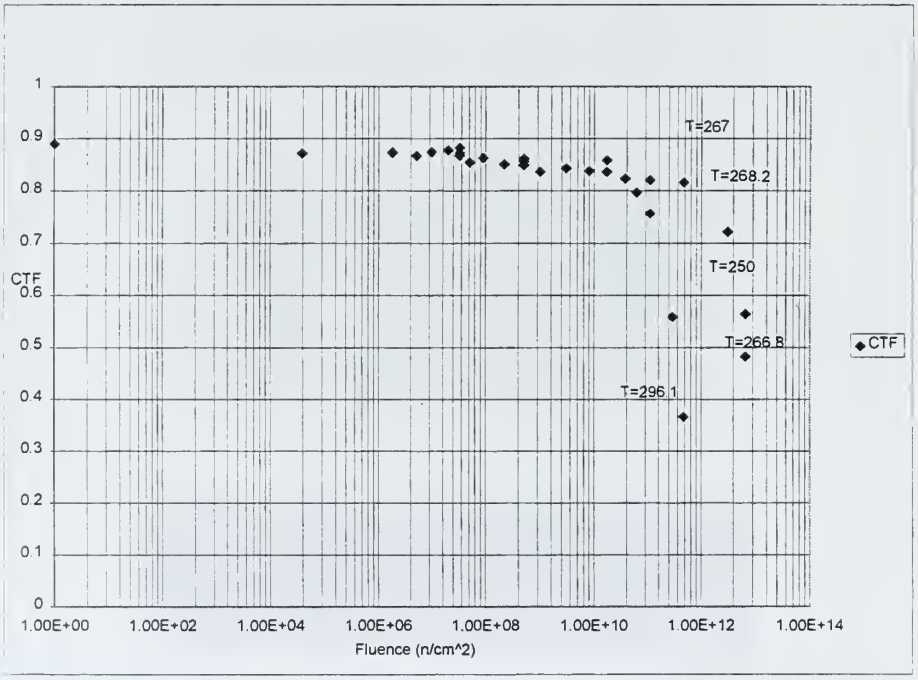

Figure 12. CTF vs. fluence from Ref [1]. Effects of temperature and dark current.

rough indication of the degradation of the resolution as the fluence increased due to the deleterious effects of increasing dark current. It also shows the positive effect of lowering the temperature.

Figure 13 shows a plot of CTF versus fluence for the images from this thesis research. The plot, created by using Eq. (1) and the same column averaging method of LT Amaden, shows that after about 10^8 n/cm^2 there is a significant degradation in the CTF. Comparing the two plots in Figures 12 and 13 shows that the CTF value goes lower from the transient effects sooner and is not affected by the camera temperature. Figure 13 indicates that average CTF is severely degraded by transient effects for neutron fluences of the sort expected for NIF.

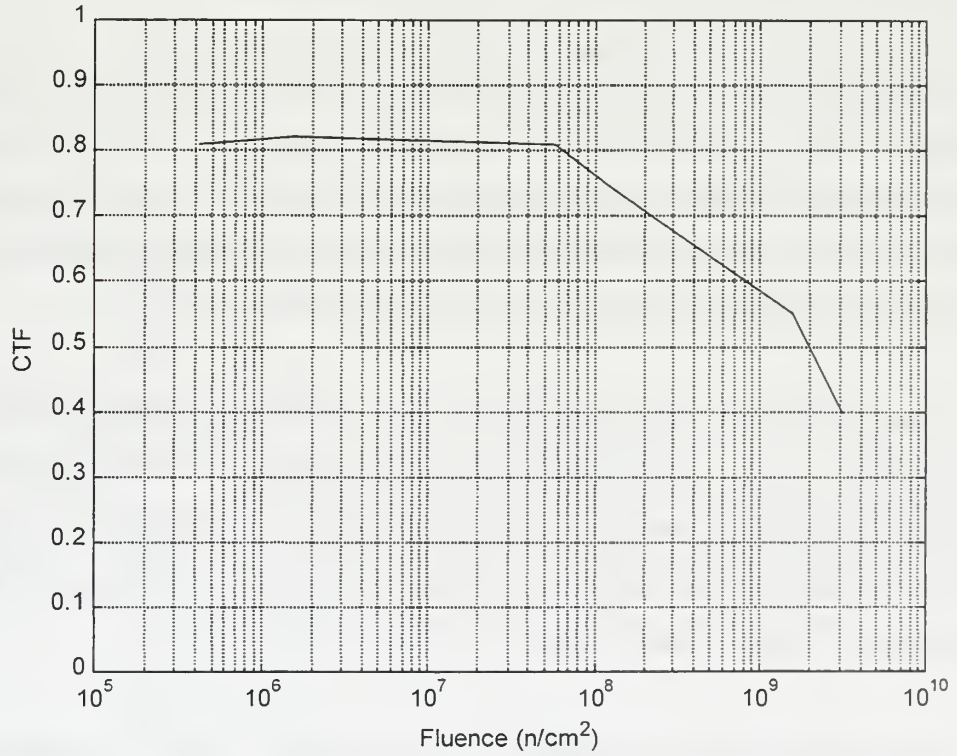

Figure 13. CTFs for simulated images. Effects of neutron stars.

While the CTF is useful for giving an average measure of how the bar pattern can be resolved from the background, this measure did not give any information on what size of detail might be completely blocked out by a star. The next section describes how the autocorrelation function was used to determine the average number of pixels effected by a neutron penetration.

E. NEUTRON "STAR" SIZE (AUTOCORRELATION)

The CTF only gave an average value for how well a bar could be distinguished from the background. If a detail in the focussed image were smaller than the pixels overexposed by a neutron passing through the detectors then there would be no guarantee that the detail would be seen. The average size of a star was determined by finding the autocorrelation of various dark images taken during irradiation.

The autocorrelation function has been used to find and average repetitive features in our images, i.e. the average size of the neutron-induced stars in an irradiated image. The autocorrelation is obtained by calculating the two dimensional Fourier transform of the image, followed by multiplying the result with its complex conjugate to get the power spectrum, and then finally performing an inverse Fourier transform [6].

The autocorrelation was computed using the commercially available *MATLAB* image processing tools [7]. An image saved in the Tagged Image File Format (TIFF) was read into *MATLAB* with the *imread* (read image) command. The functions discussed in the above paragraph were then applied to the image. Appendix B is the program used to produce the auto-correlation graphs displayed in Figures 14 and 15.

Each autocorrelogram was divided by the total number of pixels to standardize for possible comparison to images of different pixel sizes and then divided by the maximum value to normalize the vertical scale. Figure 14 shows that the average star covers up

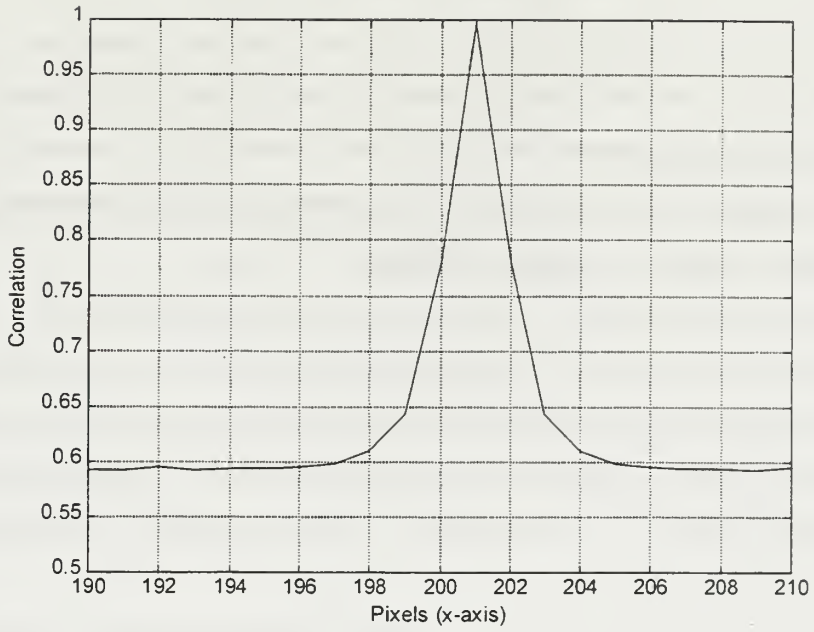

Figure 14. Irradiated image autocorrelation (horizontal).

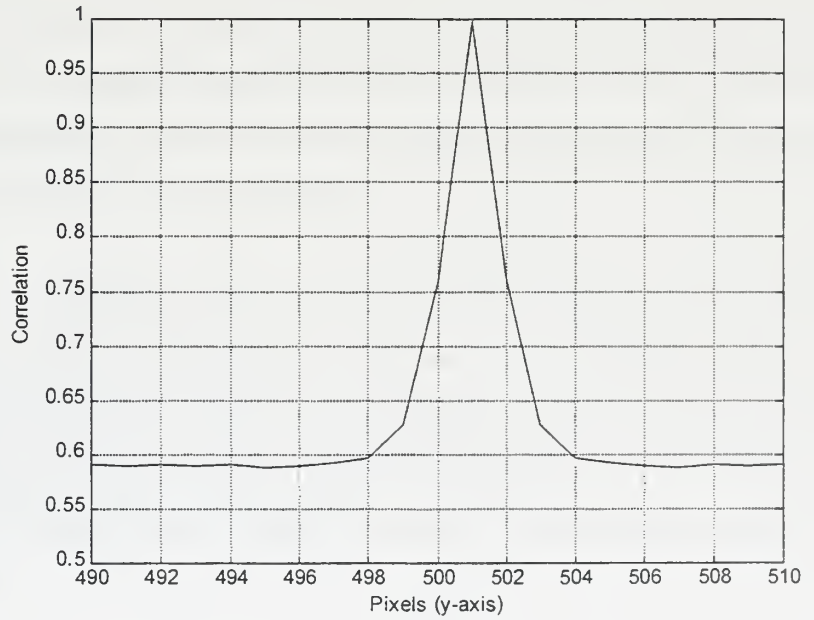

Figure 15. Irradiated image autocorrelation (vertical).

roughly 4 pixels in the x-direction and Figure 13 shows that the average star covers up about 4 pixels in the y-direction at the full width. Thus, about 16 pixels could be obscured by an average neutron-induced star. Care is needed when focussing an image on the CCD to ensure that a detail required is large enough so a 4 x 4 pixel area will not block out the detail required for a diagnostic image.

IV. CAMERA SENSITIVITY

The sensitivity of the CCD camera is a measure of how well it can convert photons to electrons. The Princeton camera used in this research has a quantum efficiency of between 30 and 40 percent in the visible wavelengths as depicted on the camera specification page included as Appendix C. About 35% of the photons are converted to electron-hole pairs (EHP). The charge is collected and is proportional to the number of photons incident upon the silicon detector. This charge is then transferred out and is attributed to the amount of light that fell onto the camera. The determination of whether camera sensitivity was damaged during the irradiation of the camera was not a transient effect, but was damage caused by permanent effects of the irradiation.

A. WHITE (ILLUMINATED) IMAGES

Images produced on the bench between periods of irradiation included those taken while the array was exposed to a uniform source of white light. I have analyzed these images to investigate if the sensitivity of the camera changed during the course of the experiment. If the digital values for the white light shown on the CCD decreased as the experiment progressed and the loss could not be attributed to other causes, then neutron irradiation may cause loss of sensitivity.

The white images used in the camera sensitivity analysis had a dark image taken from the same bench set subtracted from them to remove the dark current. In this manner the dark current caused by temperature or permanent dislocation damage should be eliminated or minimized and the sensitivity data obtained from the white images should be the result of the light flux falling on the semiconductor and not due to contributions of dark current.

B. SENSITIVITY ANALYSIS

To check for a loss of sensitivity during the course of the experiment the digital values of a white image minus dark current at very low neutron irradiation fluence would be compared to the digital values of ones taken at high neutron fluence.

After subtracting the dark current from the white image, an ROI in the center of the image was designated and *IPLab* was used to calculate a digital average for each row in the ROI. The ROI was chosen in this area to avoid saturated regions at the top and bottom. Figure 16 shows a plot of this average.

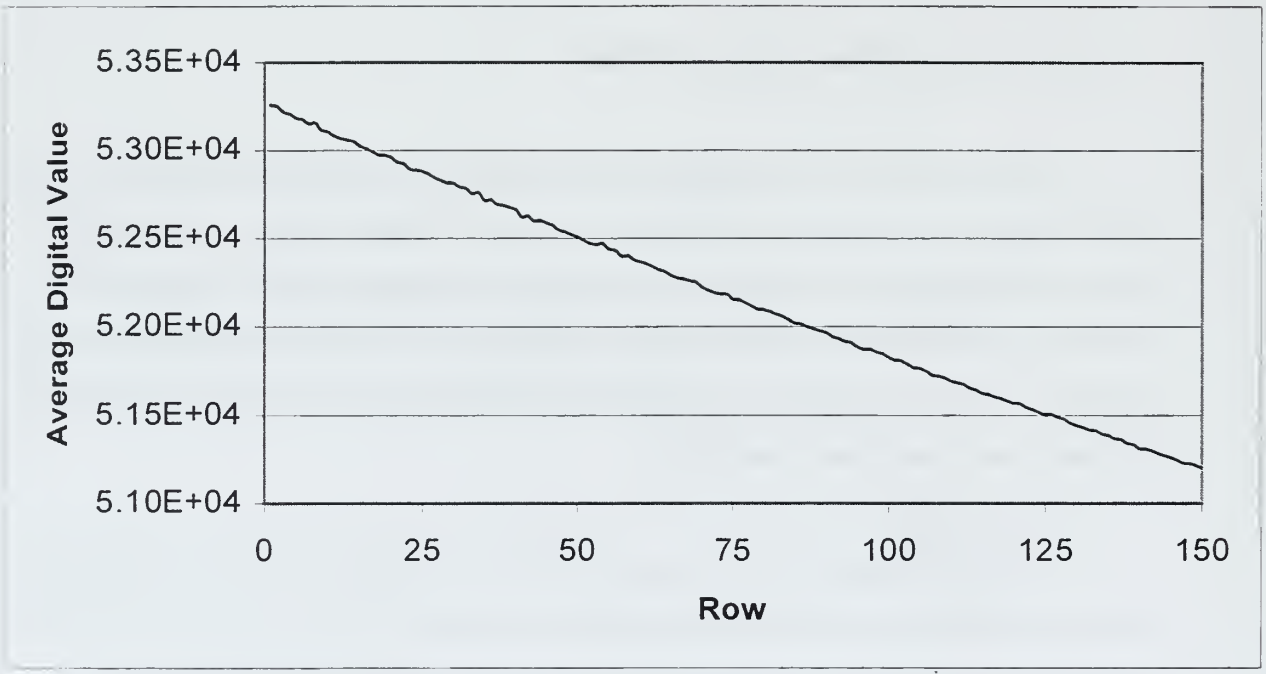

Figure 16. Average digital value vs. row. Data from illuminated bench image with dark current removed for a region of interest (ROI) including 150 rows.

The decrease in average digital value with increasing row should not be *a priori* ascribed to varying sensitivity of the camera face. Rather, the effect of CTE must be first considered. To determine the effect of CTE the high digital value in the first row was read off and multiplied by the CTE for each row until row 150 to predict a value for the low reading in the last row.

$$High\ Digital\ Value(0.99982)^{150} = Last\ Digital\ Value\ .$$

Then, if there were no sensitivity losses or other effects, the digital value at the last row should be close to the predicted value. Example:

$$5.33x10^4(.99982)^{150} = 5.18x10^4.$$

Figure 16 shows that the average digital value for the last row was $5.12x10^4$. The actual value was 600 less in the digital value than what was predicted in the above example. I am reluctant to ascribe this difference to varying camera sensitivity; inaccurate CTE seems more likely. The following equation was used to solve for the actual CTE, c_e:

$$c_e = [\frac{Low\ Digital\ Value}{High\ Digital\ Value}]^{1/150}.$$

This equation gives a CTE of about 0.99973 instead of 0.99982 found in Ref [1]. Thus CTE from Ref [1] was calculated from dark images where the signal charge and pixel loading are much less than those found in the white images.

What was apparent after comparing CTEs calculated for cumulative fluences of $4.7x10^6$, $3.9x10^7$, and $4.9x10^{10}$ n/cm^2 is that there is a slight increase in the difference

between the predicted last digital value and the actual digital value as the fluence increased. The difference respectively was about 400, 600, and 800.

This value is very small when compared to the average digital value in the images (around 50,000). It is not clear whether this small variation was due to a small loss of sensitivity or an increase in the CTI. Another possible cause of the varying digital readings was systematic variation in the output of the light source. A controlled xenon flash head with an optiliner barrel was supplying the uniform white illumination, but there was no device to measure the output of the flash to ensure each illumination was uniform.

V. CONCLUSIONS

This research confirms that CCD cameras will need to be shielded from 14MeV neutron irradiation in order for this device to be used as a diagnostic tool for fusion events at NIF. The simulated images (Figures 9, 10 and 11) show that fluences above 10^8 n/cm^2 seriously degrade the visual quality of images. Neutron fluence on the order of 10^{12} or 10^{13} n/cm^2, as would be found inside the target chamber at ranges less than 5 meters during a 21 MJ shot (Table 1), would render the image unusable.

Neutron-induced stars degraded the camera's average Contrast Transfer Function. The camera's ability to resolve a bar pattern was more degraded by neutron stars than by the increased dark current after the stars have been "cleared." This result is expected. Lowering the temperature could significantly reduce the dark current effects on CTF, but would not reduce the effects of neutron stars. CTF degradation was significant for neutron fluences greater than or equal to 10^8 n/cm^2.

The removal of dark current and the attempt to distinguish the effects of the Charge Transfer Inefficiency from a loss of sensitivity were not completely successful. After removing the dark current through image subtraction and accounting for CTI, there was still a small unexplained loss of charge. This charge loss increases slightly with fluence and could be either from a small loss of sensitivity or worsening camera CTI.

The research completed could be used to help determine how much shielding against neutron irradiation would be required to protect the camera and to allow the gathering of useful diagnostic images.

I recommend that further neutron irradiation research be conducted on a CCD camera:

1) Measure the camera's CTI prior to irradiations and after completion, as a function of CCD charge loading.
2) Repeat LT Amaden's measurements with the temperature lowered and controlled at the start and with the camera in vacuum to eliminate icing at the camera face.
3) Conduct runs with fluence levels the camera is expected to be exposed to when placed behind shielding to determine the camera's life when it is operated in a manner close to the actual anticipated use.

APPENDIX A

FLUENCE IMAGES

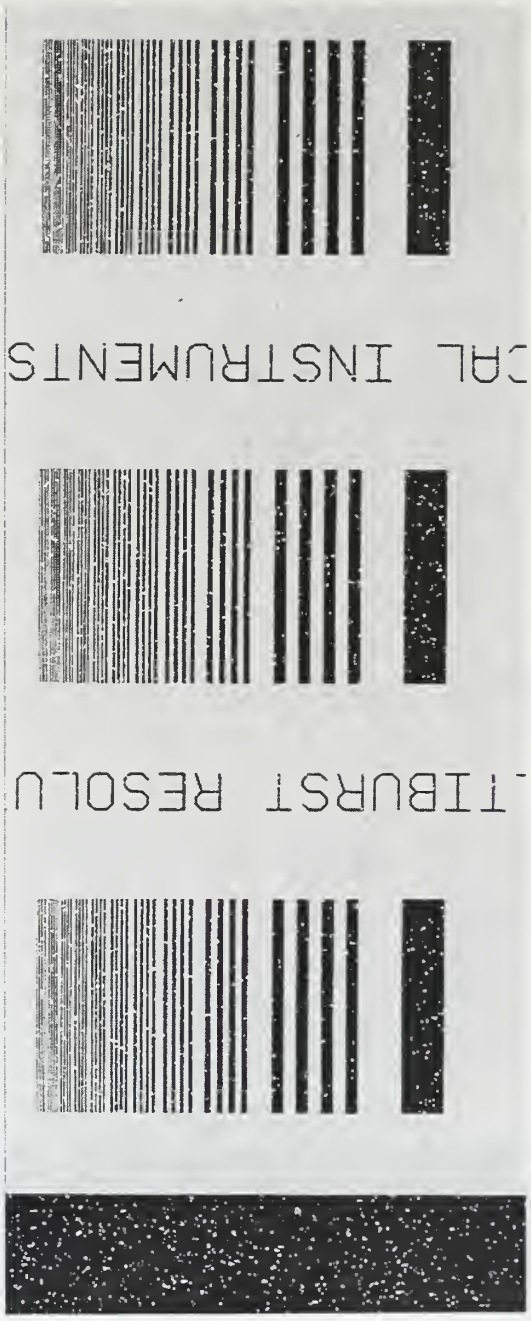

Image with fluence of 3.7×10^7 n/cm^2.

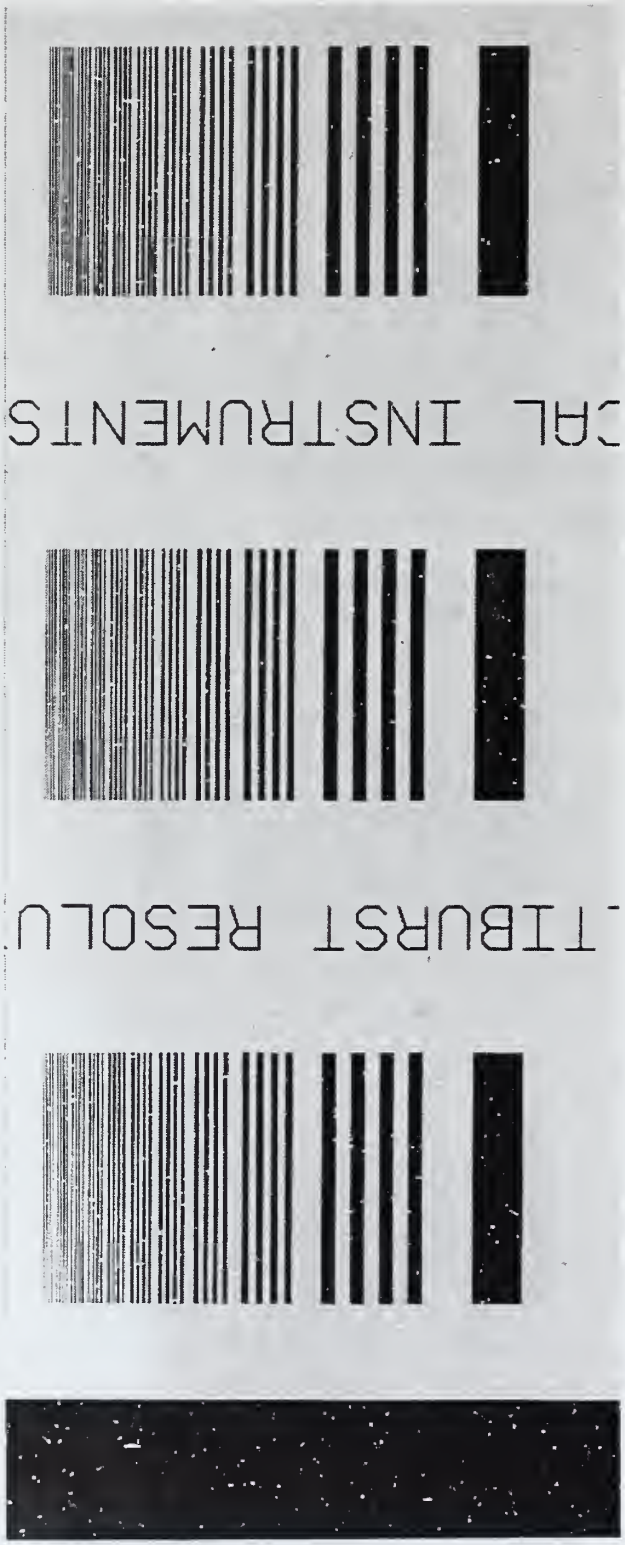

Image with fluence of 6.8×10^6 n/cm^2.

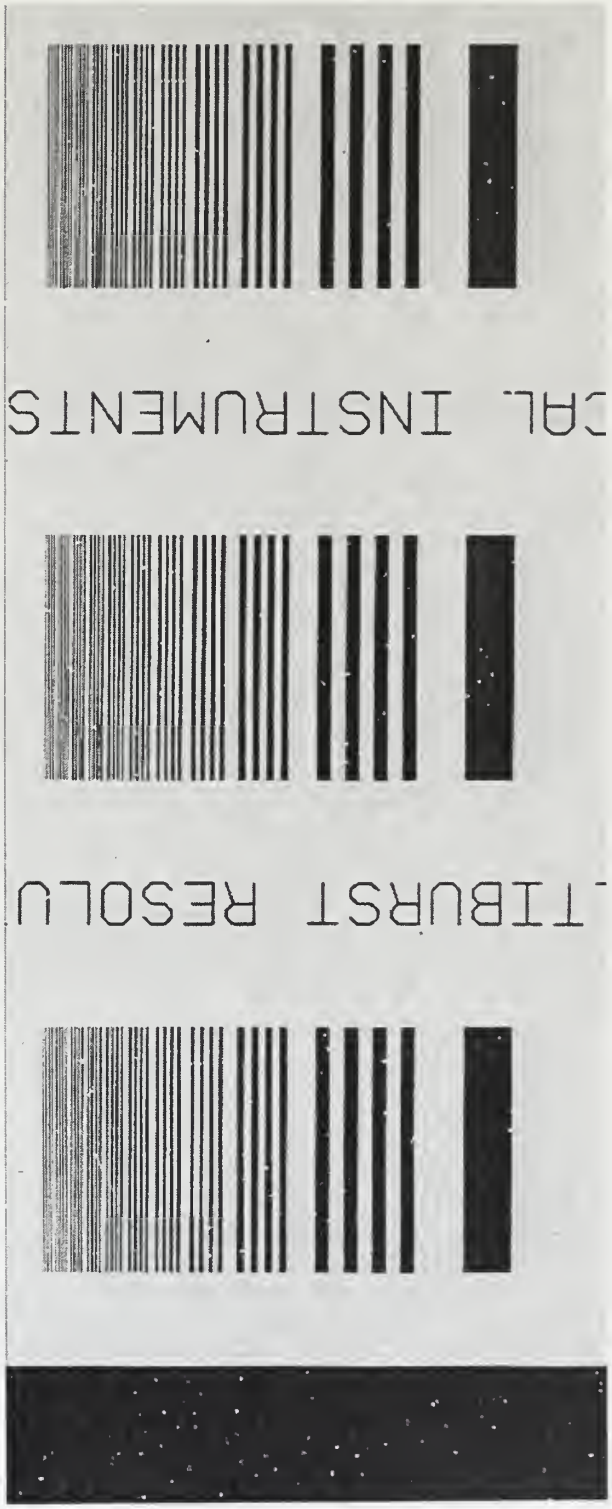

Figure with fluence of 1.6×10^6 n/cm^2.

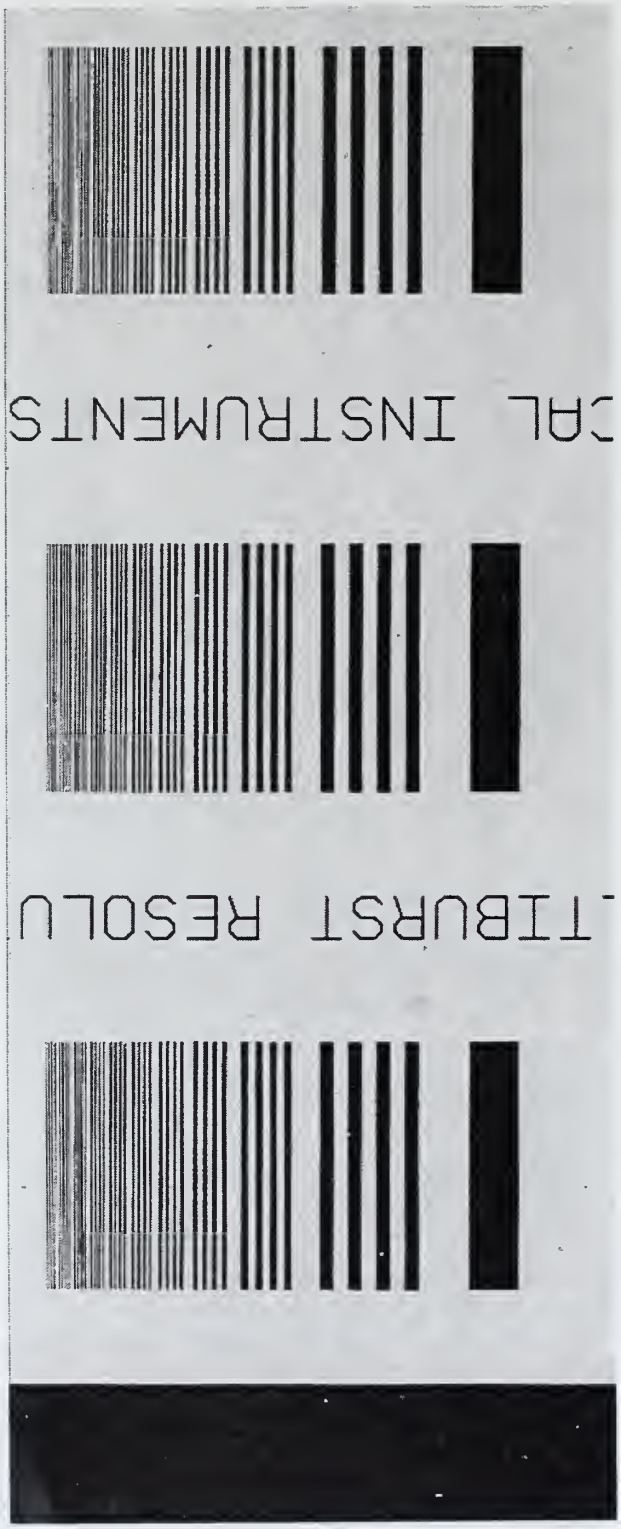

Figure with fluence of 4.33×10^5 n/cm^2.

APPENDIX B

MATLAB PROGRAM FOR CALCULATING AUTOCORRELATION

```
x=imread(a,'tif');
imagesc(x)
y=fft2(x);
figure(2)
imagesc(abs(y));
figure(3)
y2=y.*conj(y);
z=real(fftshift(ifft2(y2)));
imagesc(z)
z1=z/400000;
figure(4);
plot(z1(500,1:400));
axis([190 210 -inf inf]);
grid
figure(5)
plot(z1(1:1000,200));
axis([490 510 -inf inf]);
grid;
```

APPENDIX C

CCD Cameras

based on EEV 1152 × 1242 CCD

TE/CCD-1242E
LN/CCD-1242E

These cameras utilize large format, high pixel density (close to 1.5 million pixels) CCD arrays specifically designed for high resolution imaging. The large size pixels with their large well capacity ensures maximum light collection (with low f/# optics) and wide linear dynamic range.

When comparing slow scan CCD cameras, these are noted for the following features.

- ❑ Combination of high number of pixels and large well capacity
- ❑ Available non-MPP for maximum well capacity
- ❑ Low dark charge (MPP version)
- ❑ Full frame or frame transfer operation

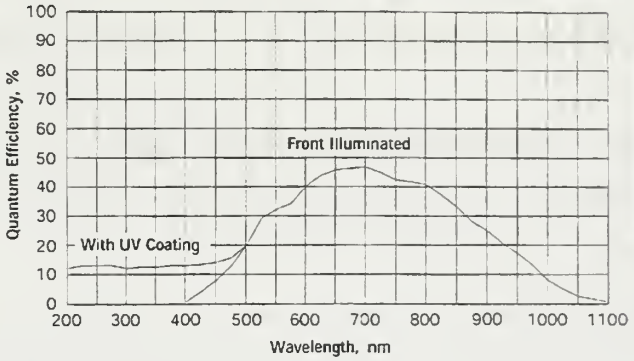

Performance Characteristics

CCD Arrays:	EEV model 05-30, standard or AIMO (MPP)
Format:	1152 x 1242, 25.9 x 27.5 mm overall, 22.5 x 22.5 µm pixels; 576 x 1242 for frame transfer, 12.9 x 27.5 mm imaging area Note that the MPP version is not recommended for most frame transfer applications due to slower vertical shifting
Full Well Capacity:	Standard, ≥ 500,000 electrons; AIMO (MPP), ≥ 300,000 electrons
Readout Noise:	4-6 electrons at 50 kHz; 25 electrons at 1 MHz
Spectral Range:	400-1080 nm; 190-1080 nm with UV-to-visible converter
Dynamic Range:	16 bits
Response Nonlinearity:	1-2% for 14-16 bits; < 3% for 18 bits
Response Nonuniformity:	≤ ±3% over entire CCD area, except blemish regions
Blemish Definitions:	Dark defects, pixels with less than 50% of the signal of surrounding pixels; Non-MPP hot defects, >10× specified average dark current; AIMO (MPP) hot defects, >100× specified average dark current; Traps are counted as dark clusters
Blemish Specifications:	43 or fewer point defects; 6 or fewer cluster defects; 2 or fewer partial column defects *or* 1 or fewer full column defects; Higher and lower grade devices are available on request, please call the factory for details
Operating Temperature:	TE/CCD, -50°C with tap water circulation, -60°C with coolant circulation, -40°C with air circulation; LN/CCD, -80°C to -140°C
Thermostating Precision:	±0.035°C over entire temperature range
Typical Dark Charge:	At -50°C, 6-8 electron/pixel-second for standard, <0.1 electron/pixel-second for MPP; At -120°C, < 1 electron/pixel-hour for standard
Scan Rate:	TE/CCD maximum scan rate is 1 MHz,

LIST OF REFERENCES

1. Amaden, C. D., *Fusion Neutron Damage to a Charge Coupled Device Camera*, Master's Thesis, Naval Postgraduate School, Monterey, California, September, 1997.
2. Wilson, J. and Hawkes, J., *Optoelectronics: An Introduction*, 3rd ed., pp. 344-348,Prentice Hall Europe, 1998.
3. Berkeley Fusion Engineering, University of California at Berkeley, Final Report, *Experimental Investigation of Neutron Damage in NIF Optics*, by E. C. Morse, 31 August 1996.
4. Hopkinson, G., Dale, C., and Marshall, P., "Proton Effects in Charge-Coupled Devices," IEEE Transactions on Nuclear Science, Vol. 43, No. 2, pp. 614-627, April 1996.
5. Stathis, P., "Radiation and EMI Effects in the NIF Environment," Lawrence Livermore National Laboratory, Livermore, California, 1 April 1994.
6. Russ, J., *The Image Processing Handbook*, 2d ed., pp. 341-346, CRC Press, 1995.
7. Littlefield, B., Hanselman, D., *Mastering Matlab: A Comprehensive Tutorial and Reference*, Prentice-Hall, 1995.